HUNGARIAN JOURNAL OF
INDUSTRY AND CHEMISTRY
Vol. 54(SI) pp. 53–62 (2026)
hjic.mk.uni-pannon.hu
DOI: 10.33927/hjic-2026-17

HUNGARIAN JOURNAL OF INDUSTRY AND CHEMISTRY
HJIC

DEVELOPMENT POSSIBILITIES OF FRICTION STIR WELDING TOOLS FOR ALUMINUM ALLOYS

EMESE GÉGÉNY[1,2] AND ZSOLT F. KOVÁCS[1]*

1 GAMF Faculty of Engineering and Computer Science, Department of Innovative Vehicles and Materials, John von Neumann University, Izsáki út 10., 6000, Kecskemét, HUNGARY
2 Doctoral School of Materials Sciences and Technologies, Óbuda University, Bécsi út 96/b, 1034, Budapest, HUNGARY

In recent years, demand for aluminum and aluminum alloys has been increasing because of their favorable properties. The properties of aluminum alloys are similar to those of structural steel, but their weight is approximately one third of that of steel. Technological development makes it possible to weld metals that are difficult to join with traditional fusion welding, such as aluminum alloys. The process is known as Friction Stir Welding (FSW). This article briefly introduces the FSW procedure and its application. In this research, 5053 aluminum alloys were welded with this technology, using customized FSW tools. These tools were manufactured using 3D printing technology, which enabled the manufacture of complex geometries. After welding, the pieces were subjected to the following material tests: visual inspection, tensile testing, hardness testing and metallographic analysis.

Keywords: friction stir welding, FSW tool, aluminum joint, welding, material testing

1. Introduction

Nowadays friction stir welding (FSW) plays a key role in metal manufacturing. It can be applied in a wide range of fields such as the aerospace industry, as well as the shipbuilding and automotive sectors. In these fields weight optimalization is a key consideration; therefore high-strength aluminum alloys have replaced structural steels. Owing to the weight reduction achieved by aluminum the technology has become widespread.

The technology was developed for welding high-strength aluminum alloys, but it has also been successfully applied to other alloys and materials such as high-strength steels, stainless steels, and titanium. The basis of the method is the creation of a solid-state bond between materials without reaching their melting point. A wear-resistant rotating tool is used for the welding process. The shoulder of the tool generates frictional heat, which reduces the strength of the workpieces without reaching their melting point. In this state, the rotating-tool moves within the material along welding line. Finally, during cooling, a solid-state bond is created between workpieces (*Figure 1*) [1]-[3].

Quality of the FSW weld seam depends on several parameters such as the pin and shoulder geometry of the FSW tool, as well as the materials [3],**Hiba! A hivatkozási forrás nem található.**,[8]. In general, FSW tools are made from tool steels that are used for welding aluminum alloys. However, welding different materials requires different tool materials. When selecting tool materials, high hardness, low reactivity with oxygen and resistance at high temperatures are required. These materials include tool steels, high speed steels (HSS), Ni alloys, metal carbides and ceramics. For each workpiece to be welded, the tool material must be selected individually to ensure appropriate weld quality. *Table 1* contains recommended tool materials for different alloys types and material thicknesses [3],[6].

The geometry of the FSW tool plays a key role in producing a high quality of welding seam (*Figure 2*). According to several studies, the FSW tool pin and shoulder affect material mixing, heat production and tool wear, too. During the process, substantial heat is generated between the tool shoulder and the workpiece. The FSW tool can be manufactured as a one-piece or two-piece design. In the latter case, the tool consists of a

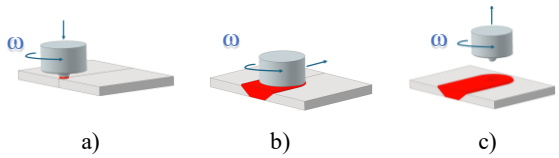

Figure 1: The bases of the FSW technology
a) Start; b) Welding; c) Finish (ω = angular velocity)

Received: 10 Nov 2025; Revised: 11 Dec 2025;
Accepted: 12 Dec 2025
*Correspondence: kovacs.zsolt@nje.hu

Table 1: The input parameters and their levels

Alloys to be welded	Material thickness (mm)	FSW tool material
Aluminum alloys	3-50	Tool steel, Co-WC composite (Cobalt-Tungsten carbide composite)
Magnesium alloys	3-10	Tool steels, WC composite
Copper alloys	3-50	Tool steels, Ni-based alloys, W-based alloys, PCBN (Polycrystalline Cubic Boron Nitride)
Titanium alloys	3-10	W-based alloys
Stainless steel	3-10	W-based alloys, PCBN
Low alloy steels	3-10	WC composite, PCBN
Nickel alloys	3-10	PCBN

shoulder and a pin with the pin being replaceable, which results in a more economical design [3],**Hiba! A hivatkozási forrás nem található.**. As the illustration in source [8] contained a conceptual error in the basic tool design, it has been corrected (*Figure 2*).

The parameters of FSW pin and shoulder depend on each other. For aluminum alloys, the diameter of the tool shoulder is 2.5-3 times larger than the diameter of the tool pin. The diameter of the tool shoulder affects heat generation and the width of weld seat [3],**Hiba! A hivatkozási forrás nem található.**.

Different shoulder sizes result different weld seam quality. According to research, the best results were achieved using tool shoulder diameters of 12 and 15 mm at a rotational speed of n=1000 rpm and a feed rate of f=600 mm/min. During the experiments, six tool shoulders with different diameters were tested and both larger or smaller diameter led to defective weld seams [27]. The FSW tool shoulder can be designed with flat, concave or convex profiles (*Figure 3a*). The flat shoulder is widely used due to its ease of manufacturing and effective heat generation. In many cases, concave and convex tool shoulders are unnecessary and time-consuming to produce. In addition, the front surface of the shoulder can be manufactured with features such as concentric circles, scrolls, grooves or a featureless surface (*Figure 3b*). These features promote more homogeneous material mixing.

The concave tool shoulder can provide better material mixing than a flat design because, during welding, the material can flow into the concave region; however, this configuration is effective only when the tool is tilted by 2-4° [10],[11].

FSW tool pin profiles play a major role in material mixing and in producing sound welds **Hiba! A hivatkozási forrás nem található.**,[13]. There are several different pin types and designs. According to studies, threaded pin designs produce high quality welds,

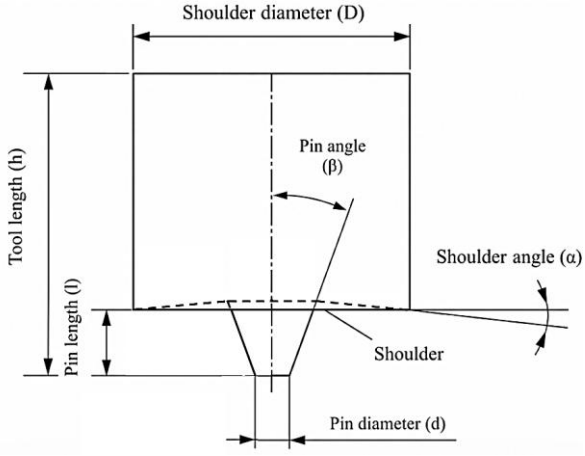

Figure 2: Main parameters of the FSW tool

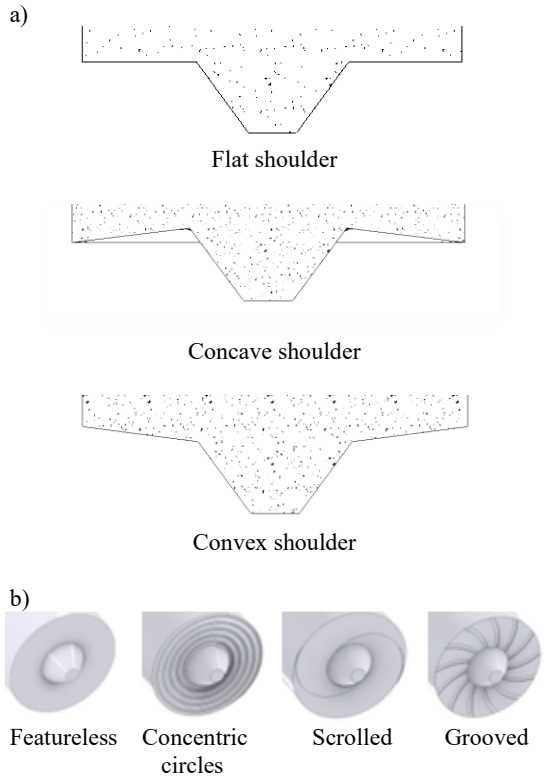

Figure 3: Types of FSW tool shoulders

whereas the non-threaded designs tend to result in defects. Welding with a smooth-surfaced conical pin produces welds of comparable quality to those made with a cylindrical threaded pin, while offering a longer tool life and lower production costs. It is worth noting that a conical pin profile generates less heat than a straight cylindrical pin profile under the identical parameters **Hiba! A hivatkozási forrás nem található.**.

According to one study, when polygonal pin profiles are compared with cylindrical designs, weld quality is consistently better with polygonal profiles. However, a disadvantage is that their manufacturing process is more complex and time-consuming [14]. A

Table 2: The recommended parameter depends on material quality, thickness, and axial force magnitude

Alloys to be welded	Material thickness (mm)	Axial force (kN)
AISI 409 M	4	24
AA2195-T6	6.35	13.8
AA6061-T6	6.35	12.5
AA7075-T6	5	8
AA6082-T6/AA7075-T6	8	12
Cu/CuZn30	3	5.5
AA2124-SiC	15	8.5
ABS	6	2

less commonly used pin geometry, the stepped cylindrical pin design, can also yield favorable results [5]. Among the required conditions is that the pin length should be shorter than the thickness of the material being welded. Effective material flow can also be ensured when the pin surface is equipped with grooves arranged in a spiral pattern with varying depths [15].

When welding thicker plates (>8 mm), it is advisable to use the so-called 'bobbin' tool, which has successfully been applied in practice to weld plates with thickness of up to 25 mm [17].

According to a study, weld quality can be optimized by increasing feed rate. An initial test was performed at a rotation speed of n=1000 rpm with a feed rate of f=100 mm/min, under which the welding seam was not appropriate. By increasing the feed rate to 437 mm/min, the seam became suitable for bending applications, and only aesthetic defects appeared on the surface **Hiba! A hivatkozási forrás nem található.**. Another study investigated the relationship between rotation speed and the heat generation using simulation. As the rotational speed increased, the temperature developed in the weld seam also increased. The temperature development simulated at a speed of 350 min-1. In this study, 1Cr11Ni2W2MoV material, which is a heat-resistant stainless steel, was welded [16].

The magnitude of the forces generated during friction stir welding (FSW) strongly depends on the material type and the thickness of the workpiece. The most important forces acting during the process are the axial force (Fz), longitudinal force (Fy), lateral force (Fx), and torque (Mz) [19]. The magnitude of these forces is a determining factor in the resulting weld quality **Hiba! A hivatkozási forrás nem található.**.

Axial force (Fz): Responsible for the friction between the tool shoulder and the workpiece, thus playing a significant role in the heat generation during the process. It also provides the necessary pressure, which contributes to the formation of a sound weld.

Longitudinal force (Fy): Helps overcome the resistance of the material being welded in the direction of the tool movement.

Lateral force (Fx): Force caused by pressure differences generated during the process. The rotational direction of the tool creates asymmetry in the material. The material in front of the tool is warmer and therefore softer, making it less resistant to the tool's forward motion. In contrast, behind the tool the temperature is lower, the material is less softened, and greater pressure is generated compared to the front side, causing tension between the two regions. This stress significantly influences tool wear and the quality of the weld. Proper parameter settings can result in longer operational time and extended tool life.

Torque (Mz): Also contributes to frictional heat generation during the process between the tool and the workpiece [19].

Numerous studies address the required axial force for a given material quality and thickness. *Table 2* summarizes the recommended parameters from one study, depending on material quality, thickness, and axial force magnitude.

The tool tilt angle is defined as the angle between the longitudinal axis of the tool and the imaginary perpendicular to the plane of the workpiece. The recommended tilt angle range is between 1-3° [15]. The determination of this angle is a critical parameter, as weld quality strongly depends on its setting. Improper adjustment of tilt angle can result in defective welds; setting the tool tilt angle is 0° is also considered incorrect In some cases, it may be justified to increase the tool inclination angle (>3°), which is why optimization should be performed prior to applying the technology [10],[20].

Another study examining friction stir welding on AA6082 aluminum, conducted at different rotational speeds (n=1000 rpm; n=1250 rpm), feed rates (f=200 mm/min; f=250 mm/min), and tool tilt angles (0°; 2°), supported the findings that welds produced at a tilt angle of 2°, a feed rate of f=200 mm/min, and a rotational speed of n=1250 rpm resulted in the smallest grain size in the weld bead, while also increasing weld hardness [22].

Friction stir welding enables the production of welds with excellent mechanical properties while being a process free of smoke, dust, and other contaminants. However, it is important to note that the technology also has certain drawbacks. These include weld defects such as tunnel defects and the so-called "lazy S" defect. This chapter focuses on the examination of welds, which enables assessment of their quality.

Through material testing, the properties of the resulting weld can be identified and evaluated. The welds are examined using the following destructive and non-destructive testing methods: visual inspection, metallographic (microstructural) analysis, tensile testing, and hardness testing. The term "lazy S" refers to a structural defect that occurs during welding. It is named after its characteristic shape, which resembles a distorted "S" and is typically observed in the central region of the welded joint. Its formation is presumably caused by aluminum oxide particles that enter the weld from the surface of the base material during the welding process [23]. This defect generally forms at the bottom of the weld and can have several causes, such as insufficient

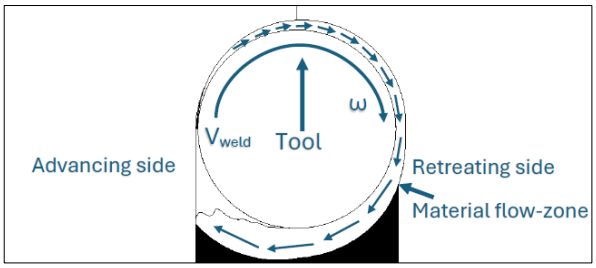

Figure 4: Material mixing around the tool (v_{weld} = welding speed, ω = angular velocity)

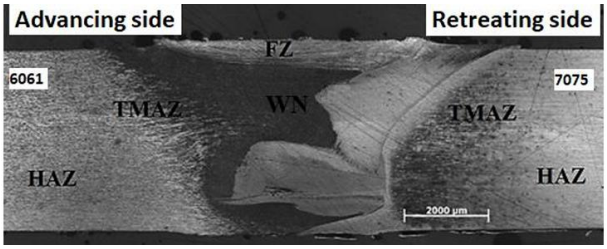

Figure 5: Cross-sectional image of the welded joint created by friction stir welding

heat input or inadequate material flow around the tool. Inclusions also negatively affect the mechanical properties of the weld [5].

During tool movement, the softened material flows around the tool, creating a so-called "advancing" and "retreating" sides due to temperature differences [3],[5]. Since material mixing is often uneven, it must be investigated through simulation and empirical methods, as improper mixing can degrade weld quality. The flow of the material around the rotating tool is illustrated in *Figure 4*. The assessment of material mixing can be performed through destructive testing, which requires preparation of the weld cross-section for metallographic analysis. The resulting cross-section demonstrates the adequacy of material mixing achieved during welding. During process setup, efforts should be made to ensure that the material mixing is as homogeneous as possible.

Figure 5 shows the structure of a welded joint produced by the friction stir welding process. The weld exhibits a fine-grained microstructure in the region traversed by the tool. Adjacent to the weld, the thermo-mechanically affected zone (TMAZ) can be observed. In this region, material flow is reduced, but the microstructure is significantly influenced not only by the temperature but also by the applied pressure. Further away, the heat-affected zone (HAZ) develops, where pressure forces no longer acts, while temperature remains an influencing factor. *Figure 5* also illustrates the intense flow zone (FZ) and demonstrates that the thermal load is not uniform on both sides of the joint, as rotational motion of the tool does not produce a uniform thermal load [3],[5],**Hiba! A hivatkozási forrás nem található.**.

2. Experimental

The aim of the research is to develop an optimal tool for the material to be welded and to identify potential variables that have not yet been investigated. The study also integrates one of the most rapidly developing manufacturing technologies of our time — 3D metal printing.

FSW tools are typically manufactured by machining (subtractive manufacturing). However, when complex pin and shoulder geometries are required, additive manufacturing becomes the preferred option. This is because additive technologies enable the production of intricate components that would be too complex to manufacture using conventional machining, offering advantages not only from a technical but also from an economic perspective.

2.1. Materials

For the experiments, a stainless steel FSW tool was used. The tools were manufactured using additive technology.

The workpieces to be welded were made of 5053 aluminum alloy, with bounding dimensions of 50 × 90 × 4 mm. The sheet dimensions were defined in accordance with the requirements of the welding apparatus. Prior to the measurements, the welding surfaces of the specimens were prepared to ensure uniformity.

The 5000 series alloys contain 0.5–5.5% magnesium, which allows their use in a wide range of applications [31]. The 5053-aluminum alloy mainly consists of aluminum and chromium, along with smaller amounts of other elements. Owing to this composition, it exhibits excellent corrosion resistance, high strength, good weldability, and favorable formability. This alloy is widely used in the marine, aerospace, and automotive industries [32].

2.2. Experimental setup

During the experiment, a total of 15 measurements were carried out at a constant rotational speed of 1000 rpm, using three different feed rates. Throughout the trials, the tool tilt angle was maintained at 0°, and no cooling was applied. Prior to the welding process, an experimental plan was developed based on the reviewed literature. The conclusions drawn from this plan were used to define the welding technological parameters, which are presented in *Table 3*.

During the welding process, the sheets were aligned in the same plane, and the joint was formed along their contact surfaces. Owing to the spiral geometry of the tool, the spindle was rotated in a counterclockwise direction to ensure that the mat6rial flow conformed to the intended tool design (*Figure 6*).

2.3. Designing of FSW tools

During the literature review, several different tool designs were identified, which served as the basis for the design of the tool pin and shoulder. With 3D metal printing, it is possible to manufacture elements with

Table 3: Welding technological parameters

Number of Measurements	Tool Name	Rotational peed (rpm)	Feed (mm/min)
1			80
2	1	1000	125
3			170
4			80
5	2	1000	125
6			170
7			80
8	3	1000	125
9			170
10			80
11	4	1000	125
12			170
13			80
14	5	1000	125
15			170

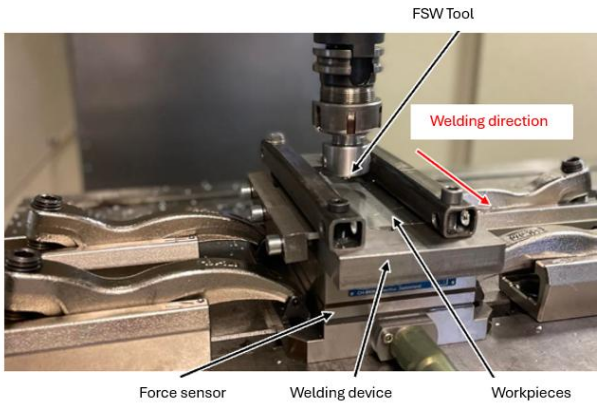

Figure 6: Experimental setup

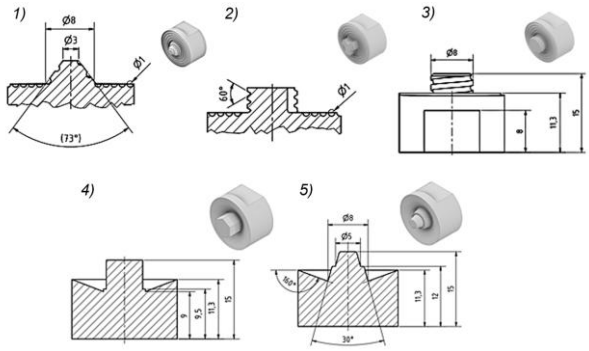

Figure 7: Designed FSW tools from 1 to 5 with dimensions

complex geometries more quickly and cost-effectively than with traditional machining [28],[29]. The design process was initiated based on the information gathered from the literature.

Firstly, the workpieces to be welded were considered, which in this case consisted of two aluminum plates with a thickness of 4 mm. The plate thickness affects the pin length, as it cannot be equal to or greater than the thickness of the material being welded. It is advisable to design the pin length to be slightly shorter to prevent it from penetrating through the material; therefore the pin length was designed to be 3.7 mm.

The next step was the determination of the shoulder diameter. The diameter of the tool shoulder significantly influences the weld bead formation. For aluminum alloys, the tool shoulder diameter is typically 2.5 to 3 times the diameter of the pin. The shoulder diameter affects both the weld bead width and the amount of frictional heat generated. In this study, all tools were designed with an identical shoulder diameter of 20 mm, however, future research should investigate the effects of varying shoulder diameters under identical process parameters.

The diameter, geometry, and the shoulder front surface and profile were designed differently for each tool (*Figure 7*). In the case of Tool 1, the shoulder has a flat desing, and its face is equipped with spiral grooves. The flat shoulder is the most common among FSW tools because, in addition to its simple design, it provides the necessary heat input. Moreover, the spiral channels on the shoulder face promote homogeneous material mixing. The tapered pin design also produced good welds in certain cases and contributes favorably to material mixing. The tapered surface was also equipped with spiral channels as well, further enhancing the mixing of materials during the welding process.

In the case of Tool 2, the shoulder design is identical to that of Tool 1, featuring a flat profile, and a face equipped with spiral grooves. However, the pin design differs. In this case, the pin does not have a tapered geometry but instead has a circular cross-section with three vertical grooves. The material flow is also influenced by the depth of the spiral channels; therefore, this aspect warrants more comprehensive investigation under specific process conditions. In addition, the spin surface was equipped with threads to further enhance material flow.

In the case of Tool 3, the shoulder design is identical to that of the first and second tools. The difference compared to the previous tool lies in the pin design. Unlike Tool 2, this tool does not feature the three vertical grooves. The material flow is ensured solely by the spiral channels on the pin and shoulder surfaces.

For Tool 4, a concave shoulder design was applied for the first time. The use of a concave shoulder may result in more favorable material flow compared to a flat shoulder design. This is because, when the tool is lowered, the material displaced by the pin enters the cavity in the tool shoulder, and as the tool moves, this material continues to flow in the direction induced by the pin. It is important to note that with a concave shoulder design, the tool must be tilted between 2° and 4° in the direction of motion relative to the workpiece surface during welding, in order to achieve good weld quality. For the pin design, a hexagonal profile was used, as

a) b) c)

Figure 8: The top view images of the welds made with Tool 1 are as follows: a) 80 mm/min; b) 125 mm/min; c) 150 mm/min

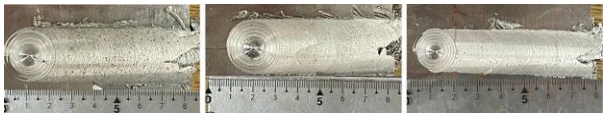

a) b) c)

Figure 9: The top-view images of the welds made with Tool 3 are as follows: a) 80 mm/min; b) 125 mm/min; c) 150 mm/min

angular profiles have a favorable effect on material flow and the mechanical properties of the weld.

For Tool 5, the shoulder profile is identical to that of Tool 4. The appropriate shoulder angle should be further investigated through empirical studies, taking the tool tilt angle into account. In this case, the pin design is tapered with a stepped configuration. Both the stepped design and the taper contribute to enhanced material mixing during the welding process.

The tools were manufactured from stainless steel using 3D metal printing on an Xact Metal 200G machine.

3. Results and experiments

This chapter presents the procedures and findings related to the testing of the welded samples. The evaluation included visual inspection, tensile testing, hardness measurements, and metallographic analysis.

The chapter does not include the material testing results of Tools 2, 4 and 5, as the poor weld quality was already evident during visual inspection.

3.1. Welding quality by visual inspection

The welds produced with Tool 1 and Tool 3 merit particular attention. The inspection process commenced with a visual examination. For the welds produced with Tool 1 at a feed rate of 80 mm/min, continuous surface scratching was observed, indicating inadequate material mixing. At a feed rate of 125 mm/min, the resulting joint exhibited a substantially improved bond; however, further increases in feed rate led to the appearance of tunnel defects within the weld (*Figure 8*).

In the case of Tool 3, a mixing weld was produced in all three trials, although surface roughness varied. At a feed rate of 80 mm/min, the weld exhibited a rougher surface; however, increasing the feed rate resulted in a gradual reduction in surface roughness. Nevertheless, defects observed in the initial section of the weld indicate the presence of tunnel-type discontinuities within the joint (*Figure 9*).

The visual inspection revealed notable differences in weld quality between Tool 1 and Tool 3. Welds produced with Tool 1 at a feed rate of 80 mm/min exhibited continuous surface scratching, suggesting insufficient material mixing and poor joint integrity. At an intermediate feed rate of 125 mm/min, weld quality improved significantly, resulting in a more coherent bond; however, at higher feed rates, tunnel-type defects became apparent, indicating limitations in process stability (*Figure 8*).

In contrast, all welds produced with Tool 3 exhibited mixing throughout the joint. However, surface roughness varied as a function of feed rate. At 80 mm/min, the weld surface was relatively rough, while increasing the feed rate progressively reduced roughness, suggesting more favourable material flow. Despite this improvement, tunnel defects were detected in the initial sections of the welds, indicating that defect formation was not entirely mitigated (*Figure 9*).

Overall, Tool 1 demonstrated sensitivity to feed rate, with optimal results observed at moderate values, while Tool 3 provided consistent mixing across all trials, albeit with surface roughness and tunnel defects influencing joint quality.

3.2. Welding quality by tensile test

For the tensile tests, three transverse specimens with a width of 10 mm were extracted from each welded joint. The nominal gauge width of the specimens was 8 mm, with a total length of 98 mm. In total, 36 specimens were prepared, corresponding to three specimens for each feed rate condition. The tensile tests were performed using an Instron 4482 universal testing machine, which provided both tabular and graphical outputs of the results.

Among the tested samples, the highest load-bearing capacity was recorded for specimens 1/125 (maximum load 7331.993 N) and 3/125 (maximum load 7109.317 N). This outcome indicates that a feed rate of 125 mm/min represents a more favorable condition for material consolidation during welding, as it provides a balance between sufficient plastic deformation and adequate heat generation. At lower feed rates (80 mm/min), excessive heat input and prolonged exposure led to surface irregularities and insufficient mixing, thereby reducing tensile strength. Conversely, at higher feed rates, reduced heat input resulted in the formation of tunnel defects, which significantly compromised joint integrity. The tensile diagrams summarizing these results are presented in *Figures 10* and *11*.

3.3. Welding quality by metallographic examination

The samples prepared by cold embedding were subjected to a three-step polishing procedure using 320, 600, and 1200 grit sandpapers. After surface preparation, the

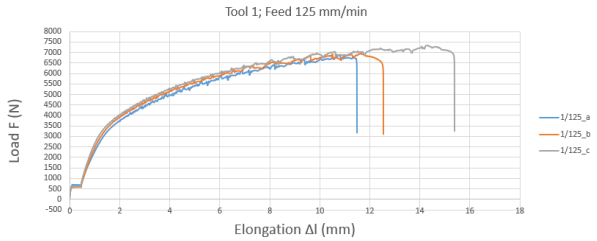

Figure 10: The tensile stress-strain diagram for the sample welded with Tool 1 at a feed rate of 125 mm/min

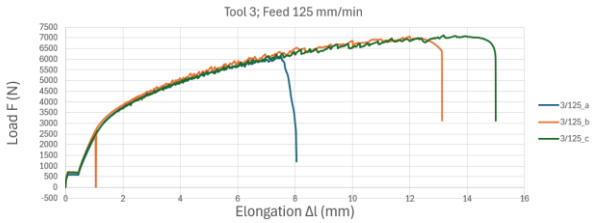

Figure 11: The tensile stress-strain diagram for the sample welded with Tool 3 at a feed rate of 125 mm/min

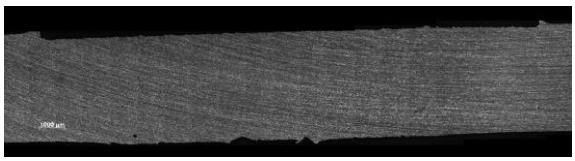

Figure 12: Cross-sectional image of the sample welded by Tool 1 at a feed rate of 125 mm/min

Figure 13: Cross-sectional image of the sample welded by Tool 3 at a feed rate of 125 mm/min

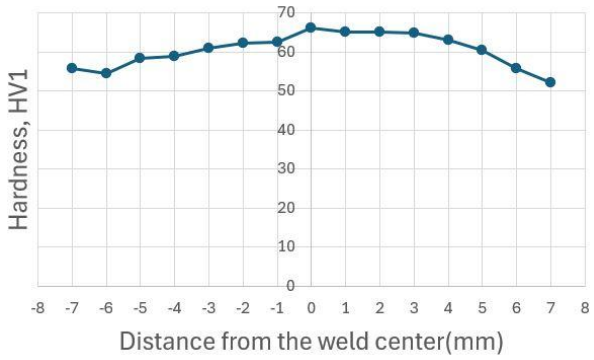

Figure 14: Hardness measurement of the sample welded by Tool 1 at a feed rate of 125 mm/min

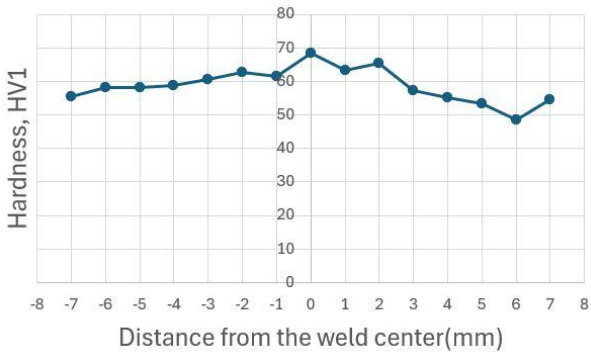

Figure 15: Hardness measurement of the sample welded by Tool 3 at a feed rate of 125 mm/min

specimens were examined under an optical microscope to identify potential defects.

The metallographic analysis revealed the presence of defects in all welds, a phenomenon commonly observed in friction stir welding of aluminum alloys. The size and morphology of these defects were strongly influenced by the feed rate and tool configuration. At the lowest feed rate (80 mm/min), prolonged interaction time caused excessive heat input, promoting turbulent material flow and resulting in larger surface irregularities and voids. At excessively high feed rates, reduced heat generation was insufficient for complete plasticization, giving rise to tunnel-type defects due to inadequate consolidation.

By contrast, the intermediate feed rate of 125 mm/min, particularly with Tool 1 and Tool 3, produced welds with the smallest defect sizes. This condition appears to provide an optimal balance between thermal input and material flow, leading to more homogeneous plastic deformation and a lower probability of defect formation. These microstructural observations are in good agreement with the tensile test results, where the 1/125 and 3/125 specimens exhibited the highest load-bearing capacity. The correlation highlights the direct relationship between defect minimization and improved mechanical performance (*Figures 12* and *13*).

3.4. Welding quality by hardness testing

Vickers hardness testing was carried out on the embedded specimens using a Struers Duramin-100 hardness tester. The analysis focused on the 1/125 and 3/125 samples, as these had demonstrated the most favorable performance in previous evaluations. A load of 1 kgf was applied during testing. Since the welded components were fabricated from the same base material, similar hardness values were anticipated across the measurement points, with a localized increase expected within the weld zone. Measurements were conducted along the crown side of the weld, progressing

horizontally from the rear side (left) toward the front side (right) (*Figures 14* and *15*).

The results confirmed the expected hardness distribution. Both samples exhibited comparable values in the base material, while a noticeable increase was observed within the weld zone, reflecting localized strengthening due to intense plastic deformation and thermal effects inherent to friction stir welding. The hardness peaks in the weld zone are consistent with the superior tensile performance and reduced defect size previously recorded for the 1/125 and 3/125 specimens. This agreement across different testing methods reinforces the conclusion that the intermediate feed rate of 125 mm/min, combined with appropriate tool geometry, provides optimal welding conditions for achieving both mechanical strength and microstructural integrity.

The experimental results demonstrated that the most promising weld quality was achieved using Tool 1 and Tool 3 at a feed rate of 125 mm/min. Both tools consistently produced joints with reduced defect size and superior mechanical properties, as confirmed by tensile and hardness testing as well as metallographic analysis. These findings suggest that further optimization of these tool designs is warranted. Future studies should focus on varying additional process parameters, particularly the tool tilt angle in the range of 1°–3°, as this adjustment is expected to enhance material consolidation and improve weld bead formation. The spiral channel design incorporated into these tools has already shown a positive influence on material flow, highlighting its potential for further refinement. Regarding Tool 2, the vertical grooves present on the probe proved detrimental under the tested conditions, as they failed to produce acceptable weld quality at any feed rate. Nevertheless, continued investigation into modified groove geometries is recommended, provided that the design enables more effective material transport during the welding process. Reconfiguring the grooves to promote controlled material flow could unlock the potential of this tool design. Overall, the evaluation highlights the strong performance of Tool 1 and Tool 3 under intermediate feed rates, while also identifying key directions for further tool development. The results underline the importance of harmonizing tool geometry and process parameters to achieve defect-free welds with favorable mechanical performance.

4. Conclusion

Friction stir welding (FSW) has become a key joining technology in modern metal manufacturing, particularly in sectors such as aerospace, automotive, and shipbuilding, where weight reduction is a primary design objective. The substitution of structural steels with high-strength aluminum alloys has accelerated the adoption of this process, as it enables lightweight structures with comparable mechanical performance.

In the present research, customized tools designed and manufactured by the author were applied to weld AA 5053 aluminum alloy plates. Welding was performed at a constant spindle speed of 1000 rpm and three different feed rates. The experimental program included visual inspections, tensile testing, hardness measurements, and metallographic analysis, providing a comprehensive assessment of joint quality. Finite element analysis (FEA) was also carried out to examine material flow around the tool, offering valuable insights for optimizing tool geometry.

The results confirmed that tool geometry exerts a decisive influence on weld formation and defect occurrence. Among the tested configurations, Tool 1 and Tool 3 operating at 125 mm/min produced the most favorable results, yielding welds with minimal defects and superior mechanical properties. These outcomes highlight the importance of spiral channels in promoting material flow, as well as the potential benefits of optimizing the tool tilt angle (1°–3°) and shoulder geometry. In contrast, Tool 2, which features vertical grooves on the probe, consistently produced unsatisfactory welds under the investigated parameters. However, modified groove geometries may warrant further exploration to improve material transport during welding.

The correlation between mechanical testing and metallographic analysis demonstrated that smaller defect sizes directly contributed to higher tensile strength and consistent hardness distribution, particularly in the 1/125 and 3/125 samples. These findings underline the importance of balancing thermal input and material flow to achieve homogeneous plastic deformation and defect-free welds.

Future research should expand on these results by refining tool geometries, investigating concave shoulder designs, and conducting further metallographic observations, including etched specimens to evaluate the heat-affected zone and material mixing. Complementary FEA simulations are also recommended to support tool development and ensure optimized material flow conditions.

- Tool geometry is a dominant factor in weld quality; Tool 1 and Tool 3 at 125 mm/min provided the best results.
- Spiral channels improve material flow and reduce defect formation.
- An intermediate feed rate of 125 mm/min balances heat input and material mixing, minimizing tunnel defects.
- Tool 2's vertical groove design is not suitable in its current form; however redesigned grooves may improve material transport.
- Hardness and tensile tests confirmed the superior performance of 1/125 and 3/125 samples, correlating with smaller metallographic defects.
- Further optimization of the tool tilt (1°–3°) and concave shoulder geometry is recommended to enhance weld bead formation.
- Future studies should include etched metallographic analysis to reveal the heat-affected zone and validate material mixing behavior.

- FEA remains a valuable tool for predicting material flow and supporting the design of optimized welding tools.

Overall, this study demonstrates that carefully engineered tool geometries, combined with optimized welding parameters, can significantly enhance the quality and mechanical performance of friction stir welded joints in aluminum alloys.

REFERENCES

[1] Hartmann, M.; Böhm, S.; Schüddelkopf, S.: Influence of surface roughness of tools on the friction stir welding process, *J. Weld. Join.*, 2014, **32**(6), 558–564, DOI: 10.5781/JWJ.2014.32.6.22

[2] Kovács, Zs.F.; Hareancz, F.: Application of friction stir welding in case of aluminium composites (in Hungarian), *Gradus*, 2021, **8**(1), 294–298, DOI: 10.47833/2021.1.ENG.011

[3] Singh, B.R.: A Handbook on friction stir welding (Lambert Academic Publishing), 2012, pp. 3–7, 69, 72–74, 90–104, ISBN: 9783659107627

[4] Beygi, R.; Galvao, I.; Akhavan-Safar, A.; Pouraliakbar, H.; Fallah, V.; da Silva, L.F.M.: Effect of alloying elements on intermetallic formation during friction stir welding of dissimilar metals: A critical review on aluminum/steel, *Metals*, 2023, **13**(4), 768, DOI: 10.3390/met13040768

[5] Meilinger, Á.: Optimization of the technological parameters of linear friction welding (PhD thesis). István Sályi Doctoral School of Mechanical Engineering, Miskolc, 2016

[6] KUKA: Friction stir welding https://www.kuka.com/en-de/products/fsw (accessed: October, 2024)

[7] Meilinger, Á.; Török, I.: The importance of friction stir welding tool, *Prod. Process. Syst.*, 2013, **6**, 25–34

[8] Bilici, M.K.: Effect of tool geometry on friction stir spot welding of polypropylene sheets, *Express Polym. Lett.*, 2012, **6**(10), 805–813, DOI: 10.3144/expresspolymlett.2012.86

[9] Srichok, T.; Pitakaso, R.; Sethanan, K.; Sirirak, W.; Kwangmuang, P.: Combined response surface method and modified differential evolution for parameter optimization of friction stir welding, *Processes*, 2020, **8**(9), 1080, DOI: 10.3390/pr8091080

[10] Dialami, N.; Cervera, M.; Chiumenti, M.: Effect of the tool tilt angle on the heat generation and the material flow in friction stir welding, *Materials*, 2019, **9**(1), 28, DOI: 10.3390/met9010028

[11] Mugada, K.K.; Adepu, K.: Role of tool shoulder end features on friction stir weld characteristics of 6082 aluminum alloy, *J. Inst. Eng. India Ser. C*, 2018, **100**(2), 343–350, DOI: 10.1007/s40032-018-0451-9

[12] Wahid, M.A.; Khan, Z.A.; Siddiquee, A.N.: Review on underwater friction stir welding: A variant of friction stir welding with great potential of improving joint properties, *Trans. Nonferrous Met. Soc. China*, 2018, **28**(2), 193–219, DOI: 10.1016/S1003-6326(18)64653-9

[13] Abolusoro, O.P.; Akinlabi, E.T.; Kailas, S.V.: Impact of tool profile on mechanical behavior and material flow in friction stir welding of dissimilar aluminum alloys, *Materialwiss. Werkstofftech.*, 2020, **51**(6), 725–731, DOI: 10.1002/mawe.202000002

[14] Kovács, P. (2021). Experimental investigation of various tools used in stir friction welding (in Hungarian) in: Research and innovation 2021 – GAMF Proceedings (GAMF Faculty of Engineering and Computer Science, John von Neumann University, Kecskemét), 2021

[15] Hossfeld, M.: Modeling friction stir welding: On prediction and numerical tool development, *Metals,* 2022, **12**(9), 1432, DOI: 10.3390/met12091432

[16] Ragab, M.; Liu, H.; Yang, G.-J.; Ahmed, M.M.Z.: Friction stir welding of 1Cr11Ni2W2MoV martensitic stainless steel: Numerical simulation based on Coupled Eulerian Lagrangian approach supports with experimental work, *Appl. Sci.*, 2021, **11**(7), 3049, DOI: 10.3390/app11073049

[17] TWI-Global: Bobbin tool friction stir welding developed https://www.twi-global.com/media-and-events/insights/bobbin-tool-friction-stir-welding (accessed: October, 2024)

[18] Oyedemi, K.; Adonyi, Y.; Anson, S.: Intermetallic effects in aluminum-to-steel friction stir weld, in: 100 years of E04 development of metallography standards, Voort, G.V. (Ed) (ASTM International), 2019, DOI: 10.1520/STP160720170209

[19] Mendes, N.; Neto, P.; Loureiro, A.; Moreira, A.P.: Machines and control systems for friction stir welding: A review, *Mater. Des.*, 2016, **90**, 256–265, DOI: 10.1016/j.matdes.2015.10.124

[20] Sun, Y.; Gong, W.; Feng, J.; Lu, G.; Zhu, R.; Li, Y.: A review of the friction stir welding of dissimilar materials between aluminum alloys and copper, *Metals,* 2022, **12**(4), 675, DOI: 10.3390/met12040675

[21] Oki, S.; Takahara, H.; Okawa, Y.; Tsujikawa, M.; Marutani, Y.; Higashi, K.: Influence of contineous transversal inclination of tool on FSW joints, *Mater. Sci. Forum,* 2007, **539-543**, 3850–3855, DOI: 10.4028/www.scientific.net/MSF.539-543.3850

[22] Laska, A.; Szkodo, M.; Koszelow, D.; Cavaliere, P.: Effect of processing parameters on strength and corrosion resistance of friction stir-welded AA6082, *Metals,* 2022, **12**(2), 192, DOI: 10.3390/met12020192

[23] Zhang, H.; Sun, Y.-M.; G., W.-B.; Cui, H.: Growth mechanism and motion trajectory of lazy “S” in friction stir welding joint of 6082-T6 aluminum alloy, *SN Appl. Sci.*, 2021, **3**(2), 278, DOI: 10.1007/s42452-021-04198-z

[24] Salih, O.S.; Ou, H.; Wei, X.; Sun, W.: Microstructure and mechanical properties of friction stir welded AA6092/SiC metal matrix composite, *Materials Sci. Eng. A*, 2019, **742**, 78–88, DOI: 10.1016/j.msea.2018.10.116

[25] Lockwood, W.D., Tomaz, B., Reynolds, A.P.: Mechanical response of friction stir welded AA2024: Experiment and modeling, *Mater. Sci. Eng. A*, 2002, **323**(1-2), 348–353, DOI: 10.1016/S0921-5093(01)01385-5

[26] Luo, J.; Wang, H.; Chen, W.; Li, L.: Study on anti-wear property of 3D printed tools in friction stir welding by numerical and physical experiments, *Int. J. Adv. Manuf. Technol.*, 2015, **77**(9-12), 1781–1791, DOI: 10.1007/s00170-014-6571-3

[27] Ramanjaneyulu, K.; Reddy, G.M.; Rao, A.V.: Role of tool shoulder diameter in friction stir welding: An analysis of the temperature and plastic deformation of AA 2014 aluminum alloy, *Trans. Indian Inst. Met.,* 2014, **67**(5), 769–780, DOI: 10.1007/s12666-014-0401-z

[28] Xact Metal: XM200G affordable metal 3D printing https://xactmetal.com/XM200G-affordable-metal-3d-printing/ (accessed: November 2024)

[29] IJAT (Department of Innovative Vehicles and Materials) https://ijat.hu/ (accessed: November 2024)

[30] Techpilot: Friction stir welding (in German) https://www.techpilot.com/de/lexikon/ruehrreibschweissen/ (accessed: January 2025)

[31] Zintilon: Types of aluminium: Properties, advantages and applications (in Hungarian) https://www.zintilon.com/hu/blog/types-of-aluminum/ (accessed: August 2025)

[32] Linsy Aluminium: Mastering 5053 aluminium: Expert tips for your project https://premiumalu.com/mastering-5053-aluminum-expert-tips-and-tricks/ (accessed: August 2025)